Geomechanics and Engineering, *Vol. 43, No. 2 (2025) 129-139*
https://doi.org/10.12989/gae.2025.43.2.129

Numerical study on snakeskin-inspired pile subjected to repetitive lateral loads

Tae-Young Kim[a], Seong-Hun Jang[b] and Song-Hun Chong*

Department of Civil Engineering, Sunchon National University, 255 Jungang-ro, Sunchon, Jeollanam-do 57922, Republic of Korea

(*Received June 18, 2025, Revised September 25, 2025, Accepted October 13, 2025*)

Abstract. Offshore monopile foundations are subjected to combined loading from waves, wind, and operational forces, which progressively degrade the surrounding soil and threaten long-term stability. Conventional approaches, such as increasing pile size or incorporating steel fins, offer enhanced stiffness but remain limited in improving resistance to cumulative lateral deformation. To address these challenges, a bio-inspired design mimicking the frictional anisotropy of snake ventral skin is proposed to enhance shaft resistance through directionally textured pile surfaces. This study investigates the long-term behavior of offshore monopile foundation equipped with snakeskin-inspired surface geometries under repetitive lateral loading. A semi-empirical numerical scheme is employed to extract stress and strains at the first cycle using the Modified Cam Clay model, and to track the progressive plastic deformation during repetitive loading using the polynomial-type accumulation function that includes volumetric strain, shear strain, and stress obliquity. Parametric analyses are performed to evaluate the influence of scale geometry (height and length) and installation orientation (cranial vs. caudal) on performance of snakeskin-inspired pile. The results show that greater scale height and shorter scale length (particularly under cranial installation) improve lateral resistance and limit displacement accumulation by enhancing load transfer efficiency. Deviatoric stress contours reveal a coupled mechanism where early-stage strain hardening transitions into localized softening, accompanied by progressive stress redistribution and displacement accumulation.

Keywords: offshore monopile foundation; repetitive lateral load; scale geometry; semi-empirical numerical scheme; snakeskin-inspired surface

1. Introduction

The extensive use of fossil fuels has accelerated the global shift toward to sustainable energy sources. Among various renewable energy sources, offshore wind energy offers significant advantages including high power generation efficiency, the resolution of land use issues, and the minimization of noise and ecological disturbance. By the end of 2023, global offshore wind capacity has reached 67.4 GW, with an additional 16.2 GW under construction (WFO 2023).

Offshore monopile foundation is subjected to combined loading from ocean waves, wind and their own operational forces. These loads induce progressive soil deformation around the foundation, which can eventually lead to excessive tilting and serviceability issues. To enhance the stability of offshore monopile foundation, traditional techniques have included increasing pile length and diameter, adopting battered piles or pile groups (Choo *et al.* 2014, Wang *et al.* 2022, Jeon and Lee 2023, Lv *et al.* 2023, Kim *et al.* 2025).

While traditional approaches have focused on modifying pile dimensions or configurations to improve foundation performance, alternative designs have been explored to enhance the frictional resistance of pile surfaces. One such example is the steel fin pile, which consists of a structural steel pile with a projecting steel plate. These fins increase the lateral and torsional load capacity by enlarging the pile's cross-sectional area and stiffness (Nasr 2014, Albusoda *et al.* 2018, Pei and Qiu 2022, Sallam *et al.* 2024). However, fin piles exhibit limited pullout resistance, as the fins primarily contribute to lateral stability rather than vertical load transfer.

Recently, bio-inspired designs derived from nature have gained attention as efficient, sustainable, and multifunctional alternatives in geotechnical engineering. Bio-inspired geotechnics seeks to emulate adaptive strategies observed in biological systems to enhance load transfer, improve anchorage, and manage deformation (Zhang *et al.* 2024). Several studies have explored diverse applications of this approach. For example, bio-inspired burrowing mechanisms mimic the penetration strategies of organisms like worms and razor clams to improve installation efficiency in soft soils (Zhang *et al.* 2023). Root-inspired anchorage systems replicate the hierarchical branching and interlocking behavior of plant roots to enhance pullout resistance and slope reinforcement (Fang *et al.* 2024, Jayashree and Sathyapriya 2025). Additionally, the ventral skin of snakes, characterized by frictional anisotropy

*Corresponding author, Professor
E-mail: shchong@scnu.ac.kr
[a]Graduate Student
[b]Undergraduate Student

ISSN: 2005-307X (Print), 2092-6219 (Online)

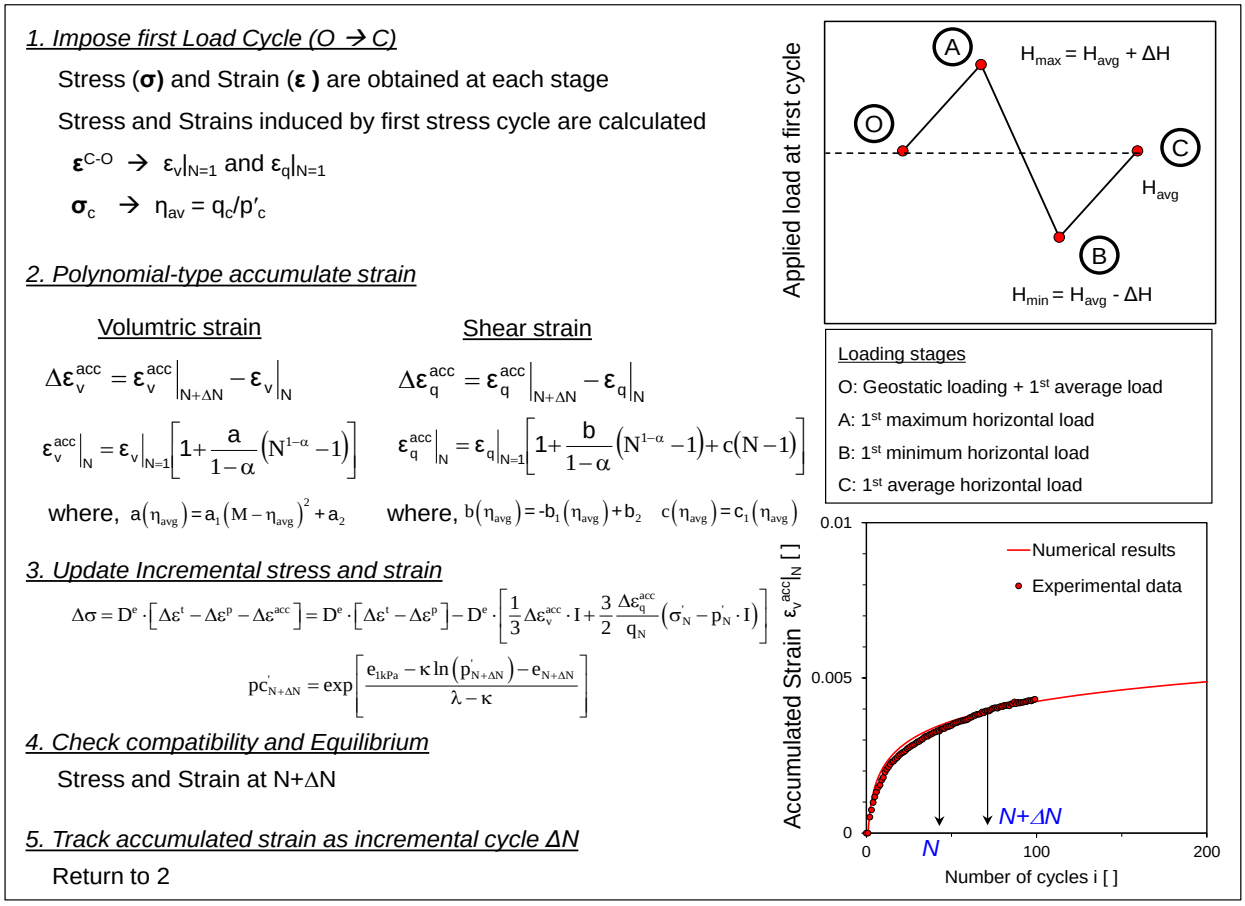

Fig. 1 Semi-explicit numerical algorithm that combines Modified Cam Clay model to extract stress and strain from the 1st loading cycle into polynomial-type strain accumulation function to track accumulated strain during repetitive horizontal loads (Modified from Chong *et al*. 2019)

induced by locomotion, which allows snakes to glide smoothly in the forward direction while generating substantial resistance in the opposite direction, has inspired the development of pile surfaces with enhanced shaft resistance (Hazel *et al.* 1999). Experimental studies have been conducted to better understand the mechanisms of load transfer at the interface between the snakeskin-inspired surface and soil. Interface direct shear tests, including both monotonic and repetitive loading conditions, were performed to evaluate the shear behavior based on scale geometry (Lee *et al.* 2023, Nawaz *et al.* 2024). In addition, penetration and pullout tests were carried out under monotonic and cyclic loading to assess the anisotropic resistance characteristics of bio-inspired pile surfaces (O'Hara and Martinez 2020, O'Hara and Martinez 2022, Kim *et al.* 2024). General observations confirm that when loading occurs in the cranial direction (i.e., against the ventral scales), higher interface resistance is observed compared to loading in the caudal direction (i.e., along the ventral scales). This anisotropic behavior suggests that snakeskin-inspired surfaces could be advantageous for installing bio-monopile in low shear resistance, as well as for mitigating lateral displacement accumulation and stiffness degradation under repetitive lateral.

This study explores the long-term soil behavior around snakeskin-inspired pile surfaces within the framework of the finite element method (FEM). A semi-empirical numerical scheme is employed to extract stress and strains at the first cycle using the Modified Cam Clay model, and to track the progressive accumulation of plastic deformation during repetitive loading using the polynomial-type accumulation function that includes fundamental features such as volumetric strain (terminal void ratio), shear strain (shakedown and ratcheting), strain accumulation rate, and stress obliquity. A series of parametric analyses are conducted by varying scale dimensions and installation direction (cranial vs. caudal). The results are analyzed to characterize the accumulation of displacement in the surrounding soil, and reveal how anisotropic surface geometry influences the stress redistribution along the pile shaft.

2. Numerical algorithm: Semi-explicit scheme

Accurate numerical modeling of long-term geostructural behavior requires tracking incremental plastic strains at each loading cycle and updating the corresponding stress responses. However, it is essential to ensure that the accumulation of physical deformation exceeds the numerical errors that occur during simulation. To address the limitations of implicit numerical schemes, previous

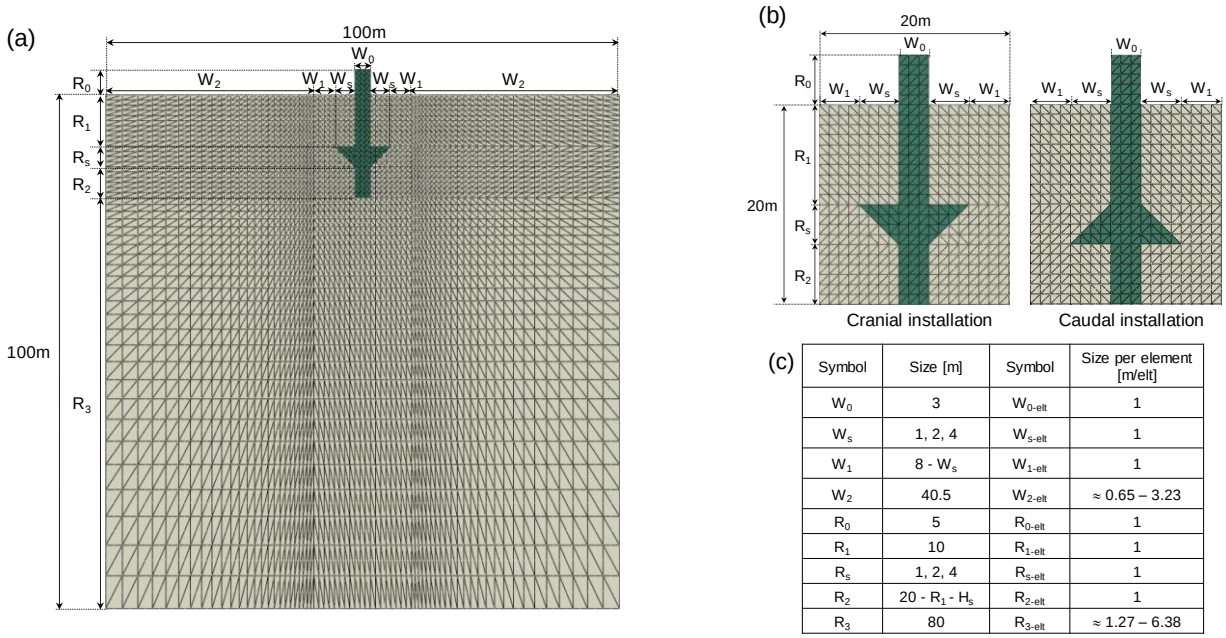

(c)

Symbol	Size [m]	Symbol	Size per element [m/elt]
W_0	3	$W_{0\text{-elt}}$	1
W_s	1, 2, 4	$W_{s\text{-elt}}$	1
W_1	8 - W_s	$W_{1\text{-elt}}$	1
W_2	40.5	$W_{2\text{-elt}}$	≈ 0.65 – 3.23
R_0	5	$R_{0\text{-elt}}$	1
R_1	10	$R_{1\text{-elt}}$	1
R_s	1, 2, 4	$R_{s\text{-elt}}$	1
R_2	20 - R_1 - H_s	$R_{2\text{-elt}}$	1
R_3	80	$R_{3\text{-elt}}$	≈ 1.27 – 6.38

Fig. 2 Generalized mesh configurations proposed in this study for snakeskin-inspired pile and surrounding soil domain: (a) full 2D mesh layout, (b) detailed mesh arrangement around pile for cranial and caudal installation and (c) dimensions and element sizes used for each mesh zone

studies have proposed semi-empirical explicit methods that embed classical constitutive models into empirical strain accumulation functions (Suiker and de Borst 2003, Niemunis *et al.* 2005, François *et al*. 2009, Kuo *et al*. 2012, Pasten *et al.* 2014). Certain forms of these accumulation functions require numerical cutoff criteria to terminate plastic strain accumulation once cyclic strain falls below the elastic threshold or when the void ratio converges to its terminal value. This process demands that strain conditions be evaluated at every load cycle across all nodes, which increases computational effort for long-duration simulations. In this study, a semi-empirical explicit approach is adopted to reproduce the long-term asymptotic trends of both volumetric and shear strains. The algorithm, implemented through UMAT subroutine in ABAQUS, is executed in two stages and summarized in Fig. 1. Previous studies calibrated the model under the zero-lateral strain condition (Chong2017) and triaxial condition (Chong *et al.* 2019), and confirmed that the simulation results show good agreement.

Step 1. Geostatic stress and the initial static load are applied to the offshore foundation using the ABAQUS platform and the Modified Cam Clay model. Sequential loading is then introduced, consisting of a maximum load, a minimum load, and the initial static load. The average static load and cyclic amplitude are determined based on the ultimate static load and a predefined safety factor. The stress and strain responses generated during the first loading cycle reflect the combined effects of the initial void ratio, initial effective stress, cyclic stress amplitude, and stress obliquity. These computed values are imposed on the nodes and elements as initial conditions for next step.

Step 2. This stage involves tracking the accumulation of volumetric and shear strains during repetitive loading. This is achieved by employing polynomial-type strain accumulation functions. These functions incorporate the fundamental characteristics of volumetric strain (terminal void ratio), shear strain (shakedown and ratcheting), strain accumulation rate, and initial stress state. At each cycle, the cumulative strains at N+ΔN are predicted and imposed on every element. The corresponding stress increment is computed from the updated strain vector defined by the plasticity model. Numerical iteration is then performed to satisfy with both strain compatibility and force equilibrium.

3. Numerical modeling of boundary value problem

3.1 Finite element mesh modeling

Mesh generation plays a critical role in the accuracy and stability of finite element simulations. The pile surface with snakeskin-inspired protrusions is required localized mesh refinement to capture the complex soil–structure interactions around the scaled geometry. In particular, arbitrarily generated mesh around the pile can introduce numerical artifacts, cause convergence issues, or lead to underestimation of localized responses. Therefore, this study proposes generalized mesh size for a snakeskin-inspired pile and its surroundings.

The overall mesh layout is presented in Fig. 2. The monopile is simulated using plane strain conditions with six-node full integration elements (CPE6). The soil domain is 100 m wide and 100 m deep, while the pile has a diameter (D) of 3 m and a total height of 25 m, including a moment arm (R) of 5 m, and an embedded depth (L) of 20 m. As shown in Fig. 2(a), the width is divided into four parts: W_0, W_s, W_1, and W_2. W_0 and W_s, which include the

Table 1 Model parameters used in this study: (a) Modified Cam Clay parameters and (b) polynomial-type strain accumulation function parameters. The parameters a, b, and c are constitutive parameters that reflect the effect of the average stress obliquity n_{avg} ($=q_{avg}/p_{avg}$) and critical state frictional state M (refer to Fig. 1). The properties of loose sand for k_o condition are adopted as detailed in Chong *et al*. (2019)

	Symbol	Value
(a) Modified Cam Clay Parameters		
Unit weight [kN/m^3]	γ	18
Isotropic compression [-]	λ	0.01
Isotropic recompression [-]	κ	0.001
Drained Poisson's ratio [-]	υ	0.3
MCC strength	M	1.42
Friction angle [^{o}]	ϕ	35
Void ratio at 1kPa [-]	e_{1kPa}	0.785
Coefficient of earth pressure at rest [-]	k_o	0.58
(b) Polynomial-type strain accumulation function		
Accumulated strain rate	α	1.14
Accumulated volumetric strain $\Delta\varepsilon_v^{acc}\|_N$	a_1	1.34
	a_2	0.5
Accumulated shear strain $\Delta\varepsilon_q^{acc}\|_N$	b_1	-6.21
	b_2	0.0
	c_1	0.0

Table 2 Snakeskin-inspired pile geometries. Pile diameter D = 3 m, Pile moment arm R = 5 m, and Pile embedded depth L = 20 m are fixed in all cases

#	Scale length l [m]	Scale height h [m]	Installation direction
1	1	1	Cranial
2			Caudal
3	2		Cranial
4			Caudal
5	4		Cranial
6			Caudal
7	1	2	Cranial
8			Caudal
9	2		Cranial
10			Caudal
11	4		Cranial
12			Caudal
13	1	4	Cranial
14			Caudal
15	2		Cranial
16			Caudal
17	4		Cranial
18			Caudal
19	Smooth		

pile and bio-inspired scale, have a consistent mesh element size of 1 m per element (m/elt). While the size of W_1 are varies according to the scale height (h), the element size within each part remains constant at 1 m/elt. W_2 is modeled using a geometric progression (0.65 to 3.23 m/elt) to obtain computational efficiency by reducing unnecessary fine meshing in the far-field region. The depth is divided into five parts: R_0, R_1, R_s, R_2 and R_3. The snakeskin-inspired

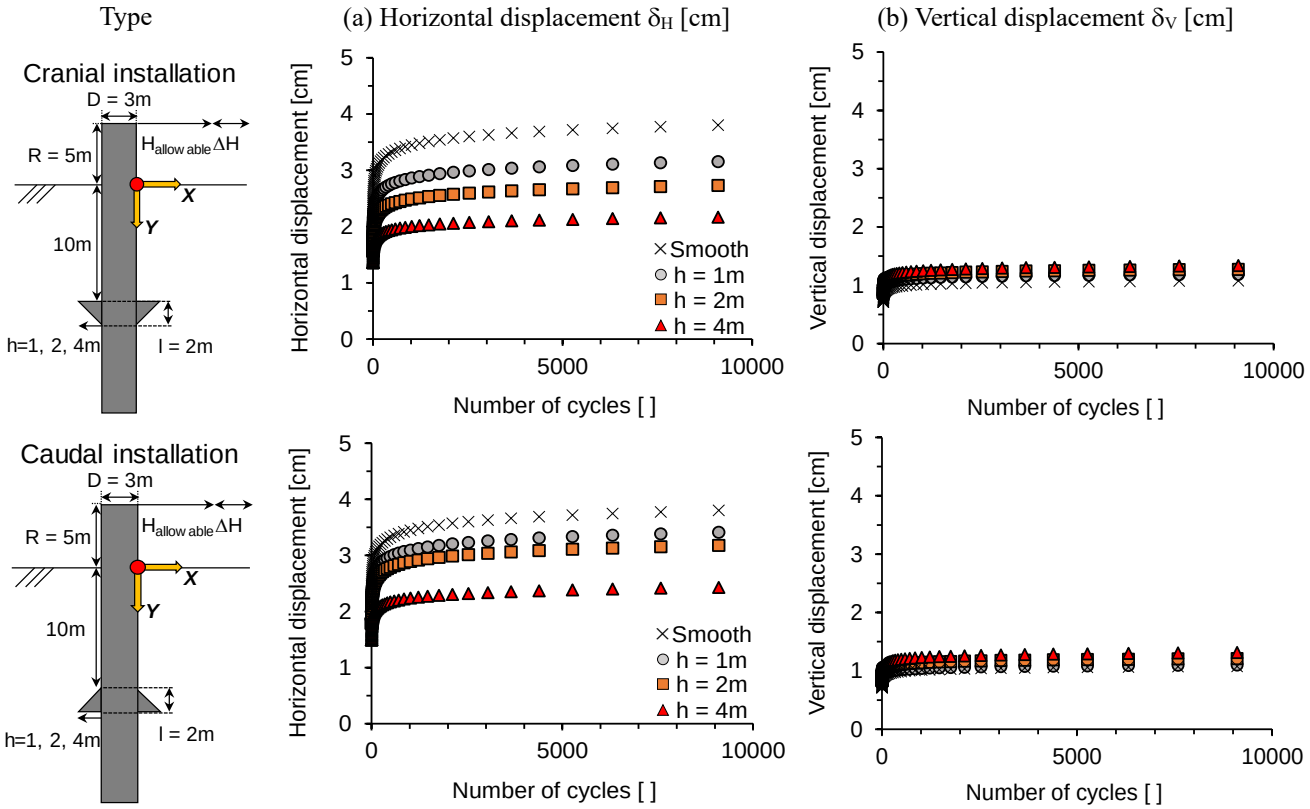

Fig. 3 Effect of scale height on the displacement evolution of a snakeskin-inspired pile: (a) Horizontal displacement and (b) Vertical displacement. The scale length l is fixed as 2 m in all cases.

pile, which composed of R_0, R_1, R_s, and R_2, maintains the same element size as the width direction (= 1 m/elt). Although R_2 various depending on the scale length (l), it consists of the same element size per elements. R_3 is generated using a geometric progression, with element sizes ranging from of 1.27 to 6.38 m/elt. In all cases, the snakeskin-inspired surfaces are designed on both side of the pile and positioned 10 m below the ground surface. To investigate the effects of frictional anisotropy on soil response, two installation orientations (cranial and caudal) are modeled, as shown in Fig. 2(b). The generalized mesh sizes modeled with a snakeskin-inspired pile and its surroundings are summarized in Fig. 2(c). The proposed mesh sizes are used for all numerical simulations.

3.2 Boundary conditions and material properties

Lateral boundaries are sufficiently placed far from the pile to satisfy semi-infinite conditions, allowing only vertical displacement, while the bottom boundary is pinned, and the top surface is free. A surface-to-surface contact function in ABAQUS is employed to model the interaction between soil and snakeskin-inspired pile under repetitive horizontal loading. In the soil-structure interaction model, the pile is assigned as the master surface due to its significantly higher stiffness, which governs the contact behavior. Conversely, the soil is designated as the slave surface, as it exhibits greater deformability due to pile movement. The tangential behavior is defined using a penalty friction formulation with an isotropic friction coefficient of 0.2 to allow controlled sliding at the interface.

The pile is modeled as a linearly elastic material, assigning concrete with unit weight (γ_{con}) of 25 kN/m^3, Young's modulus (E_{con}) of 30 GPa, and Poisson's ratio (υ_{con}) of 0.2. The model parameters are summarized in Table 1. A total of 19 cases are simulated to systematically explore the soil response with respect to snakeskin-inspired surface modifications. This study simulates ten different pile configurations, including one smooth pile and nine snakeskin-inspired piles with varying scale heights and lengths. Additionally, two installation orientations (cranial and caudal) are analyzed, as summarized in Table 2.

4. Numerical simulation of snakeskin-inspired pile

4.1 Accumulation displacement according to scale geometry conditions

The bio-inspired monopile foundation is simulated by first applying a static load, followed by a repetitive load due to the absence of the load history. The initial static load and repetitive load amplitude are determined based on the ultimate static load. Thus, the ultimate lateral load is numerically investigated under static load, followed by a monopile response to repetitive loading. In this simulation, a monopile foundation in sand is subjected to an static load ($H_{allowable}$), followed by repetitive lateral load (±ΔH). The predicted ultimate lateral load is H_{ult} = 4.1 MN. Accordingly, the average static load is set to $H_{allowable}$ = 0.68

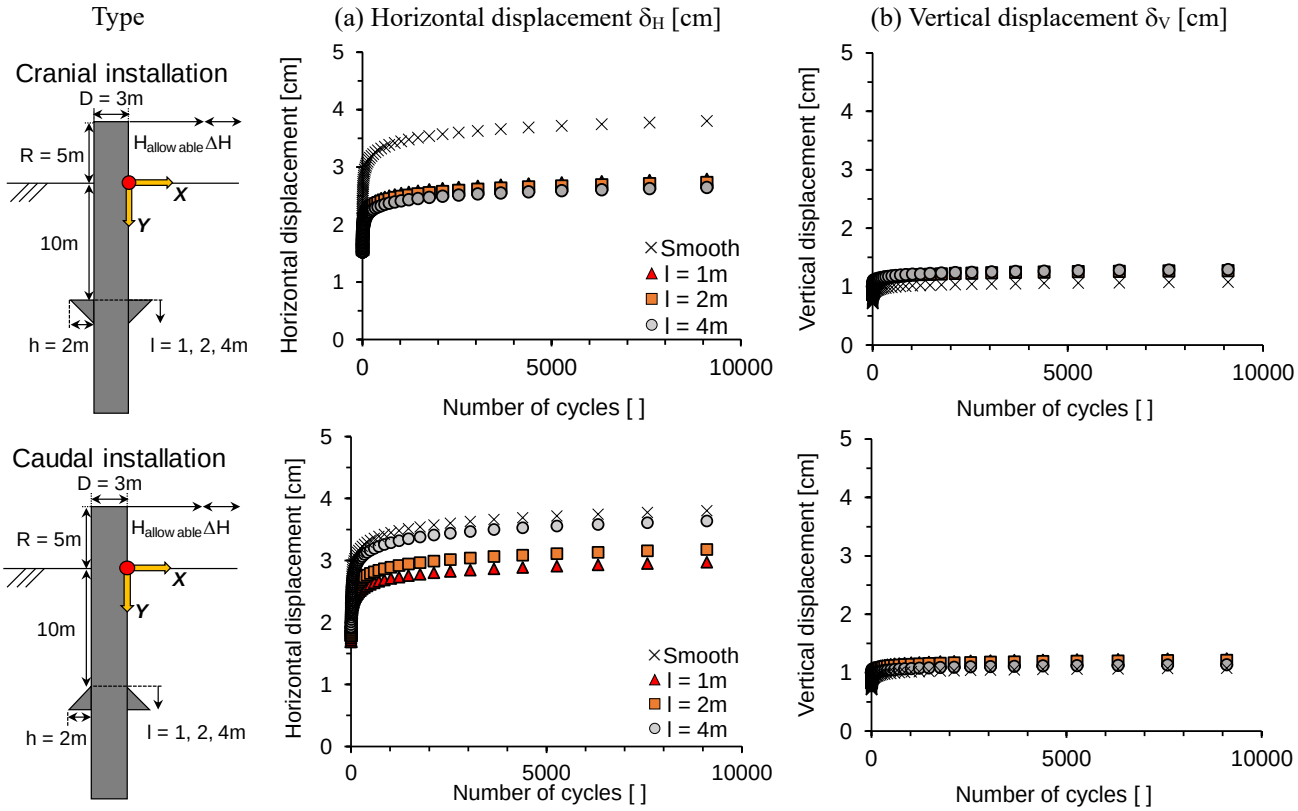

Fig. 4 Effect of scale height on the displacement evolution of a snakeskin-inspired pile: (a) Horizontal displacement and (b) Vertical displacement. The scale height h is fixed as 2 m in all cases.

MN, considering a safety factor (FS) of 6, and the cyclic load amplitude is defined as ΔH = 0.068 MN, which is 10% of $H_{allowable}$. These loads are applied at the node at pile top.

Fig. 3 illustrates the accumulated displacement behavior of bio-inspired monopiles subjected to repetitive lateral loading, comparing cranial and caudal installation orientations under varying scale heights (h = 1, 2, and 4 m). For all cases, the scale length is fixed at 2 m. A rapid increase in displacement is observed during the initial loading cycles (N < 100), after which the displacement accumulation gradually stabilizes and converges asymptotically with increasing cycle numbers. In both cranial and caudal configurations, increasing the scale height significantly reduces horizontal displacement over the number of loading cycles [Fig. 3(a)]. This reduction is more pronounced in the cranial direction, where the scale geometry promotes concentrated shearing and improved load transfer. This trend is consistent with the interface direct shear experiments conducted by Nawaz *et al.* (2024), which demonstrated that cranial shearing mobilizes higher interface friction angles and dilative response compared to caudal shearing. Compared to smooth-surfaced monopile, the addition of snakeskin-inspired surfaces notably decreases the accumulation of horizontal displacement. This suggests that the anisotropic geometry promotes better resistance against lateral loads by altering the local load transfer mechanism and increasing the effective contact area. On the other hand, vertical displacements exhibit limited sensitivity to variations in scale height and installation orientation [Fig. 3(b)]. This implies that the primary role of surface geometry is to enhance lateral resistance, with only a minor effect on vertical settlement.

Fig. 4 presents the displacement behavior of snakeskin-inspired monopiles under repetitive lateral loading, focusing on the influence of scale length l (1, 2, and 4 m) while keeping the scale height fixed at 2 m. Both cranial and caudal installation orientations are considered. As shown in Fig. 4(a), horizontal displacements consistently decrease as the scale length decreases in caudal case. This trend highlights the role of the scale edge being positioned closer to the ground surface, which mobilize greater shear resistance under lateral loading. In the cranial installation, the distance between the scale edge and the ground surface remains constant regardless of scale length. In particular, the effect of scale length is more pronounced under cranial installation, as the enhanced frictional resistance from cranial shearing dominates the response regardless of scale length. As expected, vertical displacements remain largely unaffected by scale length in both orientations [Fig. 4(b)].

The reduction in horizontal displacement observed with higher scale height and shorter scale length is attributed to enhanced shear stress mobilization and progressive strain-hardening propagating from the soil-scale surfaces. Under cranial installation, the orientation of the scales promotes forward-directed resistance during loading, intensifying plastic shearing zones and enabling more effective load transfer along the pile shaft. In contrast, caudal configurations tend to permit partial slip over the scale surface, which limits shear mobilization and results in more localized deformation near the interface.

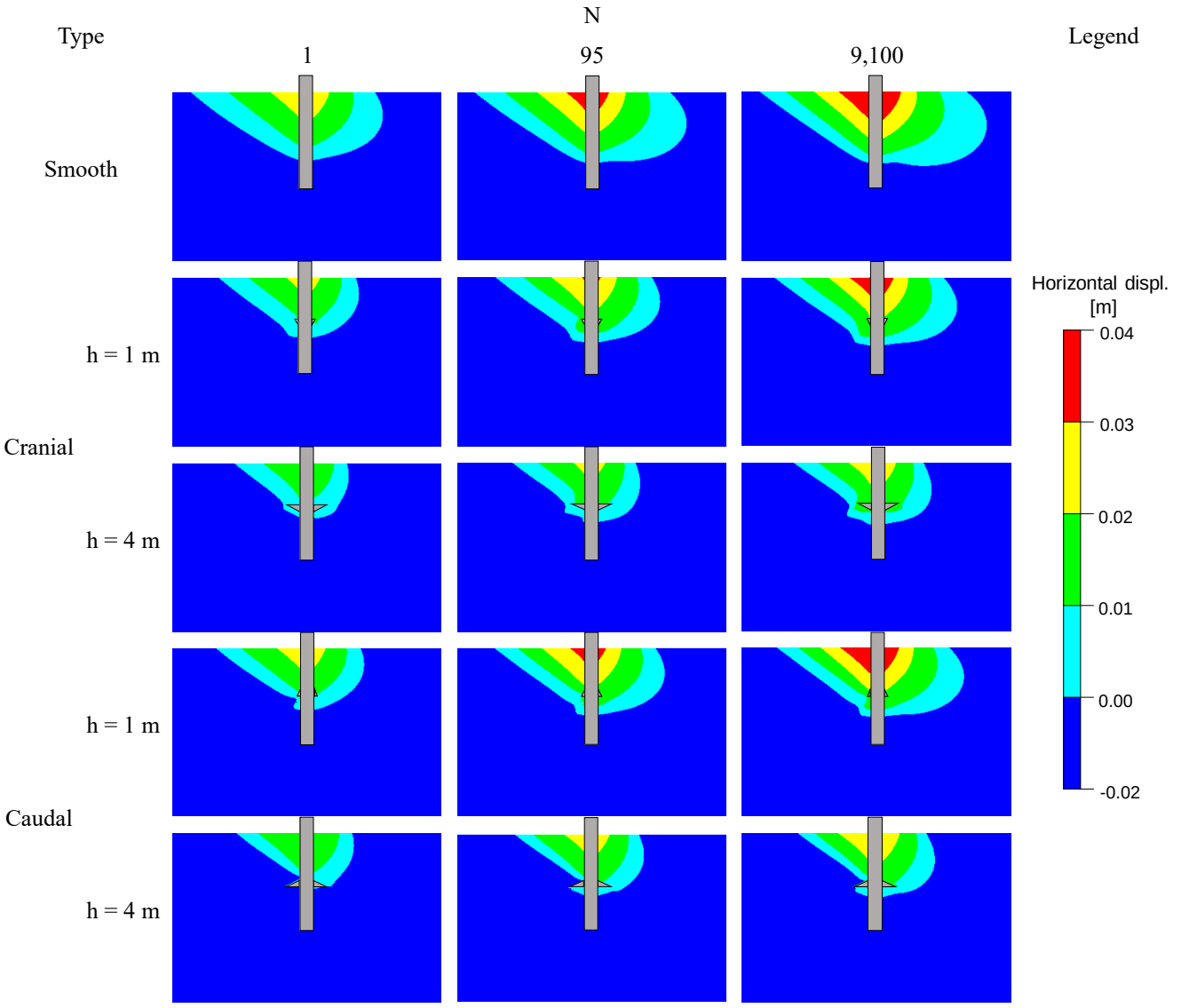

Fig. 5 Horizontal displacement contours under repetitive horizontal loading for selected cycles, showing the influence of scale height and installation orientations (Scale length l = 2 m)

4.2 Redistribution of stress and strain fields

The long-term response of snakeskin-inspired pile, including the distributions of stress and strain, is analyzed over selected loading cycles (N = 1, 95, and 9,100) and scale geometry (height and length) under two installation orientations. Fig. 5 shows the distribution of horizontal displacement in the surrounding soil of the pile according to two scale height and scale installation direction at selected domain (37 m × 59 m). The plastic displacement of the soil initially occurs at the ground surface, yet gradually extends along the pile surface down to its toe. For a smooth pile, the horizontal displacement (δ_H) is approximately 3 cm at N = 1, increasing to 4 cm at N = 9,100. The snakeskin-inspired scale significantly reduces soil deformation around pile, depending on the scale geometry and orientation. As the scale height (h) increases, the horizontal displacement reduction becomes more pronounced due to the enlarged cross-sectional interaction area between bio-inspired surface and the surround soil, regardless of scale installation direction. Furthermore, under the cranial installation, the region of cumulative displacement at a given number of loading cycles is significantly smaller than that observed in the caudal installation. In the caudal installation, the large displacement region continues to expand, resulting in a wider disturbance region in the ground.

Fig. 6 shows the distribution of horizontal displacement in the surrounding soil of the pile according to two scale length and scale installation direction. Shorter scale length minimizes the plastic deformation in caudal direction. Consistent with the previous results, the accumulative horizontal displacement under repetitive lateral loading is lower in the cranial direction compared to the caudal direction.

Figs. 7 and 8 illustrate the evolution of deviatoric stress fields surrounding the bio-inspired piles subjected to repetitive horizontal loading, highlighting the effects of scale height and scale length, respectively. Note that the

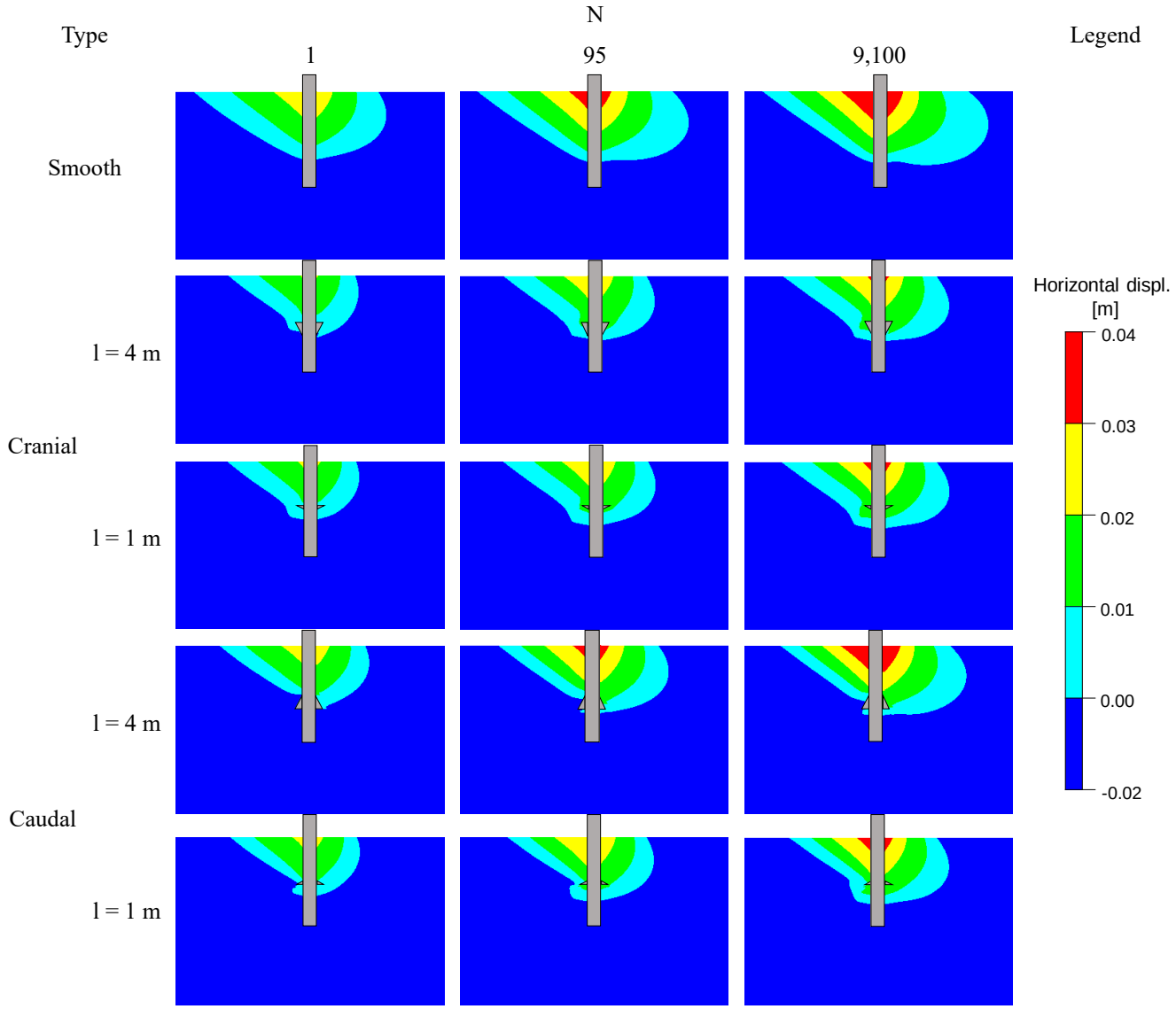

Fig. 6 Horizontal displacement contours under repetitive horizontal loading for selected cycles, showing the influence of scale length and installation orientations (Scale height h = 2 m)

deviatoric stress is directly related to shear strength response in Modified Cam Clay model. In Fig. 7, where the scale length is fixed at 2 m, the deviatoric stress patterns reveal a strong dependence on scale height. During the early loading cycles (N = 1 and 95), stress concentrations emerge near the scale tips on the loading side, reflecting localized strain-hardening. However, as the number of cycles progresses (N = 9,100), the stress magnitudes near the upper protrusions begin to relax, especially for larger scale heights. This transition toward stress redistribution and strain-softening is accompanied by enhanced stress propagation along the pile shaft and toward the pile toe. While stress concentrations continue to develop near the protrusions, they become broader and less intense, resulting in increased lateral deformation in regions where local shear resistance degrades. In Fig. 8, with the scale height fixed at 2 m, varying the scale length leads to distinct differences in stress distribution patterns. Shorter scale lengths result in more localized deviatoric stress near the upper interface, which diminishes more rapidly over the loading cycles. In contrast, longer scales induce sustained stress concentrations along the interface, particularly in the caudal orientation. These stress accumulations contribute to larger disturbed zones, consistent with the corresponding displacement fields. Overall, the results emphasize a coupled mechanism: stress concentrations due to initial strain-hardening govern the early response, while progressive strain-softening with continued cyclic shearing leads to redistributed stress and accumulated displacement.

The spatial extent and intensity of stress evolution are highly dependent on scale geometry and orientation, particularly around the tips of the protrusions, where peak stress gradually relaxes and spreads under repeated loading.

5. Conclusions

This study numerically investigates the long-term

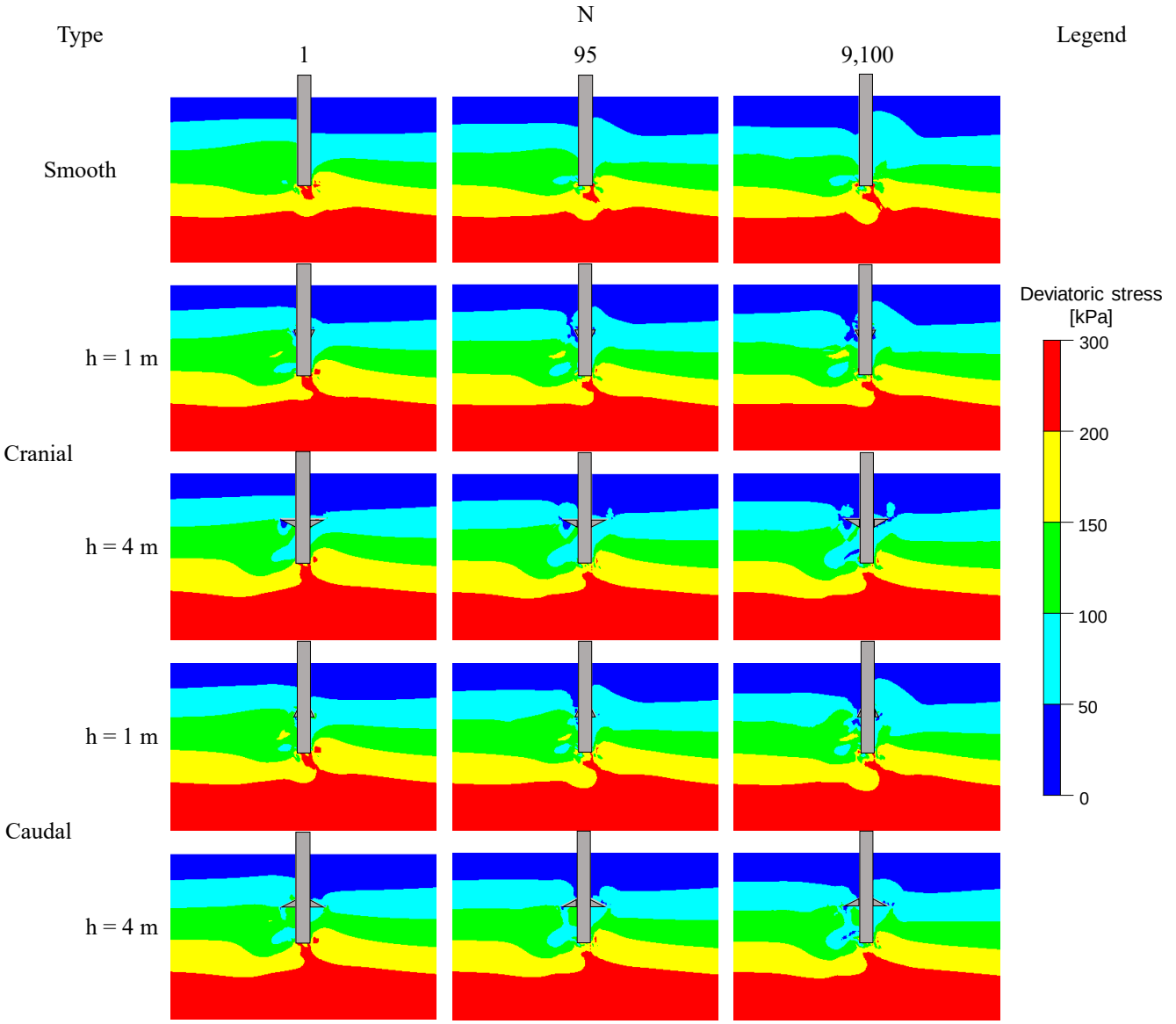

Fig. 7 Distribution of deviatoric stress under repetitive horizontal load for selected load cycles, illustrating the effect of scale height and installation orientation (Scale length l = 2 m)

behavior of offshore monopile foundation equipped with snakeskin-inspired surface under repetitive lateral loading using a semi-empirical scheme embedded with the Modified Cam Clay model and generalized mesh to reduce the numerical error for bio-inspired surface. A total of 19 cases are conducted to examine the soil response to snakeskin-inspired surface modifications, including pile configurations varying scale geometries and scale installation orientation. The main conclusions are as follows:

• Monopiles subjected to repetitive lateral loading exhibit rapid horizontal displacement during the initial cycles (N < 100), followed by a gradual convergence in displacement accumulation over the loading cycles. Meanwhile, bio-monopiles significantly reduce lateral displacement accumulation compared to smooth-surfaced piles.

• Cranial installation (against the ventral scales) mobilize less horizontal displacement around the pile compared to caudal installation (along the ventral scales), regardless of scale geometry (height and length). However, the vertical displacements remain largely unaffected according to scale geometry and orientation.

• The reduction in horizontal displacement becomes more significant with greater scale height as it increases the effective contact area with the surrounding soil in both scale orientations. The scale length induces different load transfer behaviors according to the scale installation. In caudal installation, shorter lengths mobilize increased lateral resistance, whereas in cranial installation, variations in scale length had minimal influence on the displacement accumulation.

• Under repetitive loading, plastic deformation initiates near the ground surface and progressively extends downward along the pile. In cranial installation, higher scale height helps confine plastic deformation, resulting in smaller disturbed zones in surrounding soil. It also facilitates

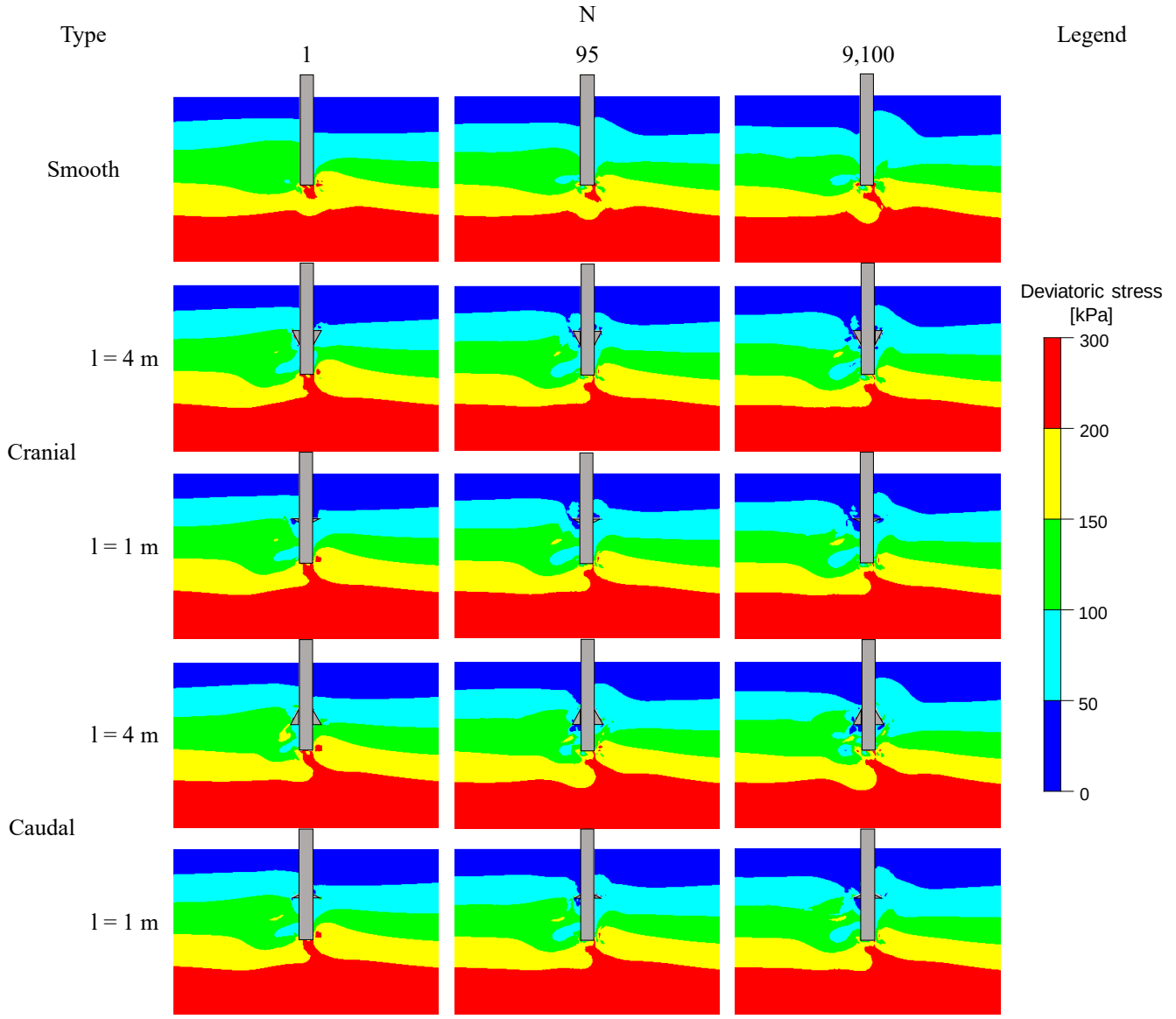

Fig. 8 Distribution of deviatoric stress under repetitive horizontal load for selected load cycles, illustrating the effect of scale length and installation orientation (Scale height h = 2 m)

broader stress redistribution and deeper propagation along the pile shaft, thereby improving load transfer efficiency. Moreover, shorter scales tend to induce more localized and transient stress concentrations near the scale tip, limiting the extent of stress redistribution.

The future study will (1) calibrate the numerical model with physical validation of the numerical results in laboratory tests, (2) evaluate the variation of penetration-pullout load transfer under groundwater conditions and different scale geometries, (3) and eventually propose optimized scale geometries for filed application.

Acknowledgments

This work was supported by the National Research Foundation of Korea (NRF) grant funded by the Korea government (MSIT) (No. 2021R1C1C1006003).

References

Albusoda, B.S., Al-Saadi, A.F. and Jasim, A.F. (2018), "An experimental study and numerical modeling of laterally loaded regular and finned pile foundations in sandy soils", *Comput. Geotech.*, **102**, 102-110. https://doi.org/10.1016/j.compgeo.2018.06.007.

Chong, S.H. (2017), "Numerical simulation of offshore foundations subjected to repetitive loads", *Ocean Eng.*, **142**, 470-477. https://doi.org/10.1016/j.oceaneng.2017.07.031.

Chong, S.H., Shin, H.S. and Cho, G.C. (2019), "Numerical analysis of offshore monopile during repetitive lateral loading", *Geomech. Eng.*, **19**(1), 79-91. https://doi.org/10.12989/gae.2019.19.1.079.

Choo, Y.W., Kim, D., Park, J.H., Kwak, K., Kim, J.H. and Kim, D.S. (2014), "Lateral response of large-diameter monopiles for offshore wind turbines from centrifuge model tests", *Geotech. Test. J.*, **37**(1), 107-120. https://doi.org/10.1520/GTJ20130081.

Fang, X., Wang, Z., Shen, C., Chen, C. and Yao, Z. (2024), "Study on the pullout bearing characteristics of root piles in coral sand

foundations under different water content states", *Appl. Ocean Res.*, **146**, 103962. https://doi.org/10.1016/j.apor.2024.103962.

François, S., Karg, C., Haegeman, W. and Degrande, G. (2009), "A numerical model for foundation settlements due to deformation accumulation in granular soils under repeated small amplitude dynamic loading" *Int. J. Numer. Anal. Meth. Geomech.*, **34**(3), 273-296. https://doi.org/10.1002/nag.807.

Hazel, J., Stone, M., Grace, M.M. and Tsukruk, V.V. (1999), "Nanoscale design of snake skin for reptation locomotions via friction anisotropy", *J. Biomech.*, **32**(5), 477-484. https://doi.org/10.1016/S0021-9290(99)00013-5.

Jayashree, J. and Sathyapriya, S. (2025), "Load sharing behaviour of bio-inspired root pile foundation in cohesionless soil under individual and combined loading conditions", *Sci. Rep.*, **15**(1), 5440. https://doi.org/10.1038/s41598-025-89168-w.

Jeon, Y.J. and Lee, C.J. (2023), "Analysis of pile group behaviour to adjacent tunnelling considering ground reinforcement conditions with assessment of stability of superstructures", *Geomech. Eng*, **33**(5), 463-475. https://doi.org/10.12989/gae.2023.33.5.463.

Kim, C., Kil, S., Kim, J., Kim, K., Kim, Y. and Moon, J. (2025), "Enhancing bearing capacity through optimal pile group spacing and arching effect", *Geomech. Eng*, **41**(1), 33-41. https://doi.org/10.12989/gae.2025.41.1.033.

Kim, T.Y., Jung, K.H. and Chong, S.H. (2024), "Development of a cone penetration testing apparatus with a textured shaft", *Appl. Sci.*, **14**(22), 10090. https://doi.org/10.3390/app142210090.

Kuo, Y.S., Achmus, M. and Abdel-Rahman, K. (2012), "Minimum embedded length of cyclic horizontally loaded monopiles", *J. Geotech. Geoenviron. Eng.*, **138**(3), 357-363. https://doi.org/10.1061/(ASCE)GT.1943-5606.0000602.

Lee, S.H., Nawaz, M.N. and Chong, S.H. (2023), "Estimation of interface frictional anisotropy between sand and snakeskin-inspired surfaces", *Sci. Rep.*, **13**(1), 3975. https://doi.org/10.1038/s41598-023-31047-3.

Lv, C.Y., Guo, Y.C., Li, Y.H., Hu-Yan, A.D. and Yao, W.M. (2023), "Experimental study on the horizontal bearing characteristics of long-short-pile composite foundation", *Geomech. Eng*, **33**(4), 341-352. https://doi.org/10.12989/gae.2023.33.4.341.

Nasr, A.M. (2014), "Experimental and theoretical studies of laterally loaded finned piles in sand", *Can. Geotech. J.*, **51**(4), 381-393. https://doi.org/10.1139/cgj-2013-0012.

Nawaz, M.N., Lee, S.H., Chong, S.H. and Ku, T. (2024), "Interface frictional anisotropy of dilative sand", *Sci. Rep.*, **14**(1), 6166. https://doi.org/10.1038/s41598-024-56621-1.

Niemunis, A., Wichtmann, T. and Triantafyllidis, T. (2005), "A high-cycle accumulation model for sand", *Comput. Geotech.*, **32**(4), 245-263. https://doi.org/10.1016/j.compgeo.2005.03.002.

O'Hara, K.B. and Martinez, A. (2020), "Monotonic and cyclic frictional resistance directionality in snakeskin-inspired surfaces and piles", *J. Geotech. Geoenviron. Eng.*, **146**(11), 04020116. https://doi.org/10.1061/(ASCE)GT.1943-5606.0002368.

O'Hara, K.B. and Martinez, A. (2022), "Load transfer directionality of snakeskin-inspired piles during installation and pullout in sands", *J. Geotech. Geoenviron. Eng.*, **148**(12), 04022110. https://doi.org/10.1061/(ASCE)GT.1943-5606.0002929.

Pasten, C., Shin, H. and Santamarina, J.C. (2014), "Long-term foundation response to repetitive loading", *J. Geotech. Geoenviron. Eng.*, **140**(4), 04013036. https://doi.org/10.1061/(ASCE)GT.1943-5606.0001052.

Pei, T. and Qiu, T. (2022), "A numerical investigation of laterally loaded steel fin pile foundation in sand", *Int. J. Geomech.*, **22**(7), 04022102. https://doi.org/10.1061/(ASCE)GM.1943-5622.0002417.

Sallam, A., Nasr, A. and Azzam, W. (2024), "Effects of simultaneous torsional and lateral loads on shaft piles with fins in sandy soil", *Geotech. Geol. Eng.*, **42**(5), 3777-3803. https://doi.org/10.1007/s10706-024-02757-w.

Suiker, A.S. and de Borst, R. (2003), "A numerical model for the cyclic deterioration of railway tracks", *Int. J. Numer. Meth. Eng.*, **57**(4), 441-470. https://doi.org/10.1002/nme.683.

Wang, X., Li, S. and Li, J. (2022), "Effect of pile arrangement on lateral response of group-pile foundation for offshore wind turbines in sand", *Appl. Ocean Res.*, **124**, 103194. https://doi.org/10.1016/j.apor.2022.103194.

WFO. (2023), "Global Offshore Wind Report", *Tech. Rep.*, World Forum Offshore Wind.

Zhang, N., Chen, Y., Martinez, A. and Fuentes, R. (2023), "A bio-inspired self-burrowing probe in shallow granular materials", *J. Geotech. Geoenviron. Eng.*, **149**(9), 04023073. https://doi.org/10.1061/JGGEFK.GTENG-11507.

Zhang, W., Huang, R., Xiang, J. and Zhang, N. (2024), "Recent advance in bio-inspired geotechnics: From burrowing strategy to underground structures", *Gondwana Res.*, **130**, 1-17. https://doi.org/10.1016/j.gr.2023.12.018.

IC